

# Morphology of the Interaction Between the Stream and Cool Accretion Disk in a Semi-detached Binary Systems

D.V. Bisikalo<sup>1</sup>, A.A. Boyarchuk<sup>1</sup>, P.V. Kaygorodov<sup>1</sup>, O.A. Kuznetsov<sup>1,2</sup>

<sup>1</sup>Institute of Astronomy, Russian Academy of Sciences, Moscow, Russia

<sup>2</sup>Keldysh Institute of Applied Mathematics, Moscow, Russia

2003

## Abstract

We analyze heating and cooling processes in accretion disks in binaries. For realistic parameters of the accretion disks in close binaries ( $\dot{M} \simeq 10^{-12} \div 10^{-7} M_{\odot}/year$  and  $\alpha \simeq 10^{-1} \div 10^{-2}$ ), the gas temperature in the outer parts of the disk is  $\sim 10^4$  K to  $\sim 10^6$  K. Our previous gas-dynamical studies of mass transfer in close binaries indicate that, for hot disks (with temperatures for the outer parts of the disk of several hundred thousand K), the interaction between the stream from the inner Lagrange point and the disk is shockless. To study the morphology of the interaction between the stream and a cool accretion disk, we carried out three-dimensional modeling of the flow structure in a binary for the case when the gas temperature in the outer parts of the forming disk does not exceed 13 600 K. The flow pattern indicates that the interaction is again shockless. The computations provide evidence that, as is the case for hot disks, the zone of enhanced energy release (the “hot line”) is located beyond the disk, and originates due to the interaction between the circum-disk halo and the stream.

## 1 Introduction

In 1999-2002, we developed a three-dimensional, gas-dynamical model and used it to study the flow patterns in binary systems [1–14]. These studies indicate that the flow structure is substantially affected by rarefied gas of the intercomponent

envelope. In particular, a self-consistent solution does not include a shock interaction between the stream from the inner Lagrange point  $L_1$  and the forming accretion disk (a “hot spot”). The region of enhanced energy release (the “hot line”) is located beyond the disk and is due to the interaction between the envelope and the stream. However, these solutions were obtained for temperatures of the outer parts of the accretion disk of 200 000 – 500 000 K. To check if this behavior is universal, the morphology of the flow must be considered for various disk temperatures.

First, we will study here the interval of plausible temperatures of accretion disks in close binaries. In Section 2, based on an analysis of heating and cooling in accretion disks, we will show that, for realistic parameters of the disks in close binaries, ( $\dot{M} \simeq 10^{-12} \div 10^{-7} M_\odot/\text{year}$  and  $\alpha \simeq 10^{-1} \div 10^{-2}$ ), the gas temperature in the outer parts of the disk is between 13 600 K and  $\sim 10^6$  K. This implies that cool accretion disks can form in some close binaries.

Second, we will consider the morphology of the interaction between streams of matter and cool accretion disks in semi-detached binary systems (Sections 3 and 4). The basic problem here is whether the interaction between the stream and the disk remains shockless, as was shown for relatively hot disks [1, 3, 4, 8, 14]. Section 5 presents our main conclusions and a physical basis for the universal nature of the shockless interaction between the stream and disk.

## 2 Heating and Cooling in Accretion Disks

In this Section, we consider the temperature of an accretion disk for various accretion rates, i.e., the dependence  $T(\dot{M})$ .

### 2.1 Basic Equations

The vertical structure of an accretion disk is specified by the balance between the vertical component of the gravitational force and the (vertical) pressure gradient, which, in turn, is specified by the balance between heating and cooling of the gas. The heating is associated with viscous dissipation of kinetic energy, and also with bulk radiative heating, which, in turn, is specified by the radiation of the central object. Cooling is brought about by several mechanisms: bulk radiative cooling, radiative heat conduction, and convection. Assuming that advective terms and terms associated with adiabatic heating or cooling are small, the steady-state energy equation

$$Q^+ - Q^- = 0$$

can be written as follows.

(1) For the optically thin case, when  $Q^+$  is specified by bulk radiative heating and viscous heating and  $Q^-$  is determined by bulk radiative cooling,

$$Q_{visc}^+(\rho, T) + n^2 \cdot (\Gamma(T, T_{wd}) - \Lambda(T)) = 0. \quad (1)$$

Here,  $\Gamma(T, T_{wd})$  is the radiative-heating function, which depends on the gas temperature  $T$  and the temperature of the central object  $T_{wd}$ ,  $\Lambda(T)$  is the radiative-cooling function, and  $Q_{visc}^+(\rho, T)$  is the viscous heating.

(2) For the optically thick case,  $Q^+$  is specified by viscous heating, while  $Q^-$  is specified by radiative heat conduction<sup>1</sup> and convection in the vertical direction:

$$Q_{visc}^+(\rho, T) - \frac{\partial F_{rad}}{\partial z} - \frac{\partial F_{conv}}{\partial z} = 0. \quad (2)$$

Here,  $F_{rad}$  and  $F_{conv}$  are the radiative and convective energy fluxes. To determine the functions in (1) and (2), we will need

– the equation of continuity

$$-\dot{M} = 2\pi \int r \cdot \rho \cdot v_r \, dz = \text{const}, \quad (2)$$

– the equation of angular-momentum balance  $\lambda \equiv r^2 \Omega_K$  in the radial direction:

$$\frac{\partial}{\partial r} (r \cdot \rho \cdot v_r \cdot \lambda) = \frac{\partial}{\partial r} \left( \nu \cdot \rho \cdot r^2 \cdot \frac{\partial \Omega_K}{\partial r} \right), \quad (3)$$

from which it follows that

$$|v_r| = -\nu \cdot \Omega_K' \cdot \Omega_K^{-1} \cdot r^{-1} \simeq \nu \cdot r^{-1}, \quad (4)$$

– and the viscous heating

$$Q_{visc}^+ = \rho \cdot \nu \cdot \left( r \cdot \frac{\partial \Omega_K}{\partial r} \right)^2. \quad (5)$$

Here,  $\dot{M}$  is the accretion rate,  $\Omega_K = \sqrt{GM/r^3}$  the angular velocity of the Keplerian rotation of the disk,  $M$  the mass of the central object,  $G$  the gravitational constant,  $\rho$  – the density,  $v_r$  the radial velocity, and the  $\nu$  – coefficient of kinematic viscosity. Note that the molecular viscosity cannot provide the necessary

---

<sup>1</sup>We neglect molecular heat conduction since it is very small compared with the radiative heat conduction.

dissipation, and dissipation processes are usually considered to be associated with turbulent or magnetic viscosity.

To determine the vertical pressure gradient, we will use the equation of hydrostatic balance in the vertical direction

$$\frac{1}{\rho} \cdot \frac{\partial P}{\partial z} = \frac{\partial}{\partial z} \left( \frac{GM}{\sqrt{r^2 + z^2}} \right) \simeq -\Omega_K^2 z, \quad (6)$$

as well as the equation of state of an ideal gas with radiation

$$P = \rho \mathcal{R}T + \frac{1}{3}aT^4.$$

Here,  $P$  is the pressure,  $T$  the temperature,  $\mathcal{R}$  the gas constant, and  $a$  the radiation constant. All equations are given in cylindrical coordinates,  $(r, z)$ .

## 2.2 The Solution Method

To determine the dependence  $T(\dot{M})$ , we will use (2) and (4) together with the expression for the viscosity coefficient. We will use the formula for suggested by Shakura [15],  $\nu = \alpha c_s H$ , where  $H$  is the height of the disk and  $c_s \simeq \sqrt{\mathcal{R}T + \frac{1}{3}aT^4/\rho}$  is the sound speed. If we neglect the  $z$  dependence of the density and use  $\bar{\rho}$  averaged over the height (further, we will denote this quantity simply as  $\rho$ ), the integration of (6) yields the height of the disk  $H$ :

$$H = c_s \cdot \Omega_K^{-1}.$$

We will determine  $c_s$  from the temperature in the equatorial plane of the disk,  $z = 0$ . This approach is sufficiently correct for our purposes due to the uncertainty in the parameter  $\alpha$ . As a result, we obtain an equation relating  $\dot{M}$ ,  $T|_{z=0}$ , and  $\rho$  for the specified  $r$  and  $\alpha$ ,

$$\dot{M} = 2\pi \cdot \alpha \cdot \Omega_K^{-2} \cdot \rho \cdot c_s^3 = 2\pi \cdot \alpha \cdot \Omega_K^{-2} \cdot \left( \mathcal{R}T\rho^{2/3} + \frac{1}{3}aT^4\rho^{-1/3} \right)^{3/2}. \quad (7)$$

This equation reduces to a cubic equation in the variable  $\rho^{1/3}$ , and its solution has two branches: one with a negative real root and two complex ones, and one with three real roots, one of which is negative. Only positive real roots for the density are physically meaningful. For such roots to exist, the following condition must be satisfied:

$$\dot{M} > \frac{\sqrt{3}\pi \cdot \sqrt{\mathcal{R}} \cdot a \cdot \alpha \cdot T^{9/2}}{\Omega_K^2}. \quad (8)$$

which yields the minimum accretion rate for the given  $T$ ,  $r$ , and  $\alpha$ . When deriving this condition, we used the equation of state taking into account the radiation pressure.

This estimate can also be written in the form

$$T < 7 \cdot 10^5 \left( \frac{r}{R_{wd}} \right)^{-2/3} \left( \frac{\dot{M}}{10^{-9} M_{\odot}/year} \right)^{2/9} \left( \frac{\alpha}{0.1} \right)^{-2/9} \text{ K},$$

where  $R_{wd} = 10^9 \text{ cm}$  is the radius of the accretor (white dwarf).

Let us consider the condition (8) for the outer parts of the accretion disk. Let us take  $r = A/5$ , where  $A$  is the distance between the components of the binary  $A = 1.42 R_{\odot}$ , which corresponds to situation for the dwarf nova IP Peg; as a result, we obtain

$$\dot{M} > 10^{-9} \left( \frac{T}{10^5 \text{ K}} \right)^{9/2} \left( \frac{\alpha}{0.1} \right) M_{\odot}/year. \quad (9)$$

If (8) is satisfied, the roots of Eq. (7) relating  $\rho$ ,  $T$ , and  $\dot{M}$  for a given  $r$  and  $\alpha$  can be written

$$\rho = (\mathcal{R}T)^{-3/4} \left( \frac{\dot{M}\Omega_K^2}{2\pi\alpha} \right) \sin^3 \left( \frac{1}{3} \arcsin \left( \sqrt{\mathcal{R}a} T^{9/2} \frac{2\pi\alpha}{\dot{M}\Omega_K^2} \right) \right),$$

$$\rho = (\mathcal{R}T)^{-3/4} \left( \frac{\dot{M}\Omega_K^2}{2\pi\alpha} \right) \cos^3 \left( \frac{1}{3} \arcsin \left( \sqrt{\mathcal{R}a} T^{9/2} \frac{2\pi\alpha}{\dot{M}\Omega_K^2} \right) + \frac{\pi}{6} \right)$$

(for simplicity, we have omitted numerical factors  $\sqrt{3}/2 \simeq 1$ ). The first of these corresponds to disks with dominant radiation pressure ( $\beta = \frac{1}{3} a T^4 / \rho \mathcal{R} T > 1$ ) and the second to disks with dominant gas pressure ( $\beta < 1$ ).

These formulas describe the two branches of the two-parameter dependence  $\rho(\dot{M}, T)$ . To calculate the dependence  $T(\dot{M})$ , we must use the additional heat balance equations (1)–(2). As follows from Section 2.1, the form of (1)–(2) depends on the optical depth of the disk, which, accordingly, must be calculated.

### 2.3 Optical Depth

The optical depth  $\tau$  is specified by the product of the absorption coefficient  $\kappa$ , the density, and the geometrical depth of the layer  $l$ :  $\tau = \kappa \cdot \rho \cdot l$ . For disk accretion, the basic parameter is the ratio of the geometrical depth of the layer where  $\tau = 1$  and the height of the disk:  $l^{\tau=1}/H$ . After simple manipulation, we obtain

$$\frac{l^{\tau=1}}{H} = \frac{2\pi \cdot \alpha}{\kappa \cdot \dot{M}} \cdot c_s^2 \cdot \Omega_K^{-1}. \quad (10)$$

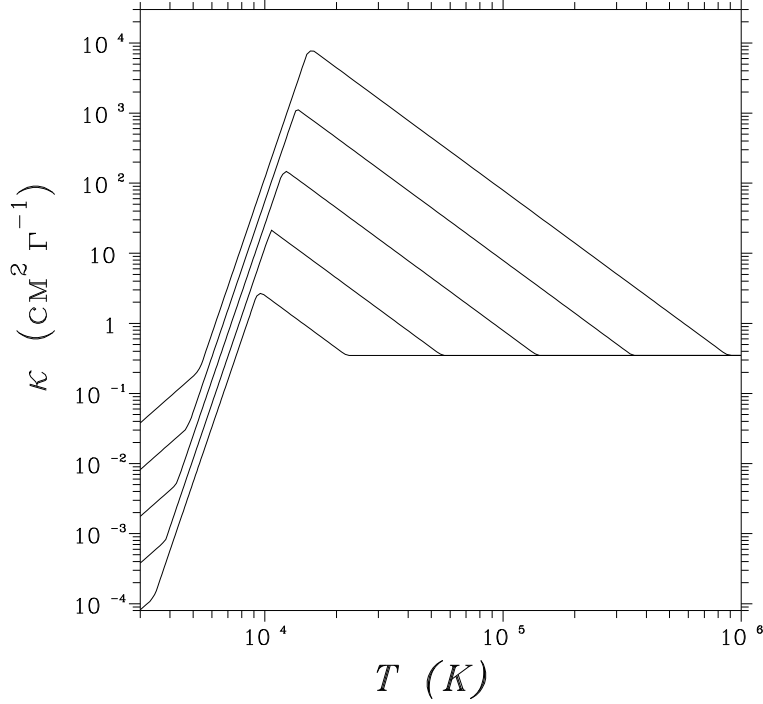


Figure 1: The  $\kappa(T)$  dependence for  $n = 10^{18} \text{ cm}^{-3}$ ,  $n = 10^{17} \text{ cm}^{-3}$ ,  $n = 10^{16} \text{ cm}^{-3}$ ,  $n = 10^{15} \text{ cm}^{-3}$ , and  $n = 10^{14} \text{ cm}^{-3}$  (top to bottom) [18].

The absorption coefficient  $\kappa$  displays a complicated dependence on  $T$  and  $\rho$  (and also on the degree of ionization, chemical composition, etc.). Here, we adopted the simple approximation for  $\kappa(T, \rho)$  [16–18]

$$\kappa(T, \rho) = \begin{cases} \kappa_1 \cdot \rho^{2/3} \cdot T^3, & \kappa_1 = 10^{-8}, & (\kappa_1) \\ \kappa_2 \cdot \rho^{1/3} \cdot T^{10}, & \kappa_2 = 10^{-36}, & (\kappa_2) \\ \kappa_3 \cdot \rho \cdot T^{-5/2}, & \kappa_3 = 1.5 \cdot 10^{20}, & (\kappa_3) \\ \kappa_4, & \kappa_4 = 0.348. & (\kappa_4) \end{cases}$$

According to [18], these four subregions correspond to scattering on molecular hydrogen, scattering on atomic hydrogen, free–free and free–bound transitions, and Thompson scattering. The boundaries of the sub-regions, i.e. the transitions from one expression to another, are specified by the equality of the  $\kappa$  values calculated from these expressions. Figure 1 presents the dependences of  $\kappa$  on  $T$  and  $\rho$ . We can see regions with  $d\kappa/dT > 0$ , where thermal instability can develop when the dependence between the surface density and the disk temperature forms

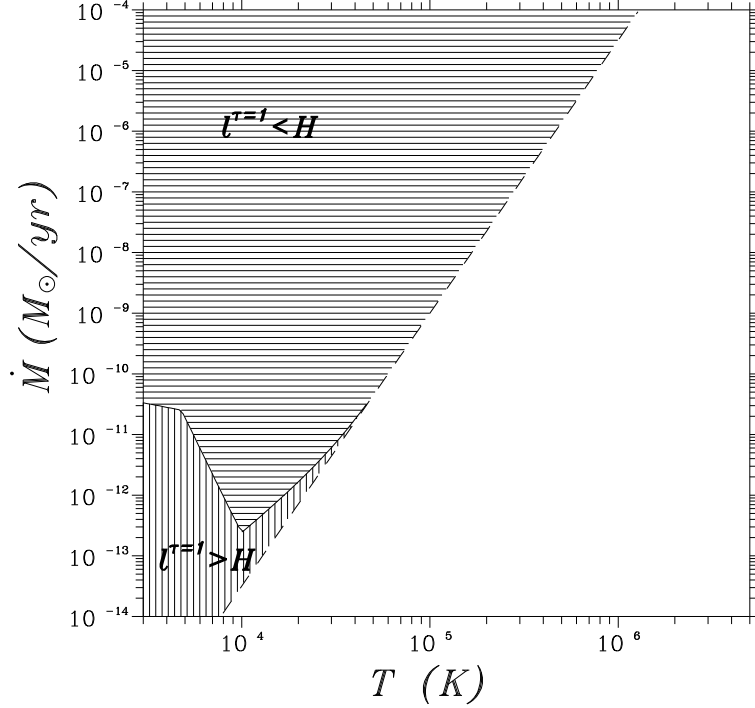


Figure 2: Solution of (7) for disks with dominant gas pressure in the  $(T, \dot{M})$  plane for  $\alpha = 0.1$  and  $r = A/5$ . The horizontal thick shading indicates optically thick disks, and vertical shading optically thin disks; the solid line marks the border between these regions. The dashed line corresponds to condition (9) for the existence of the solution of (7); there is no solution below this line.

an S curve in the  $(\Sigma, T_{eff})$  plane. Thermal instability is often invoked to explain the phenomenon of dwarf novae (see, for example, [19, 20]); however, it is clear that this can occur only for sufficiently cool disks.

Let us return to (7), taking  $\alpha = 0.1$  and  $r = A/5$  and considering disks with dominant gas pressure, for which  $\beta = 1/3aT^4/\rho\mathcal{R}T < 1$ . The shaded region in the  $(T, \dot{M})$  plane in Fig. 2 corresponds to all possible solutions for these disks. The dashed line corresponds to condition (9) for the existence of a solution for (7) – there is no solution below this line. The solid line indicates the boundary between the optically thick and optically thin solutions: the horizontal shading marks the region of optically thick disks, while the vertical shading marks optically thin disks. Figure 3 presents a similar pattern for disks with dominant radiation pressure ( $\beta > 1$ ).

We can see from Fig. 2 that, for realistic values  $\dot{M} \in [10^{-12}, 10^{-7}]M_\odot/\text{year}$ , disks with dominant gas pressure are mainly optically thick, though solutions cor-

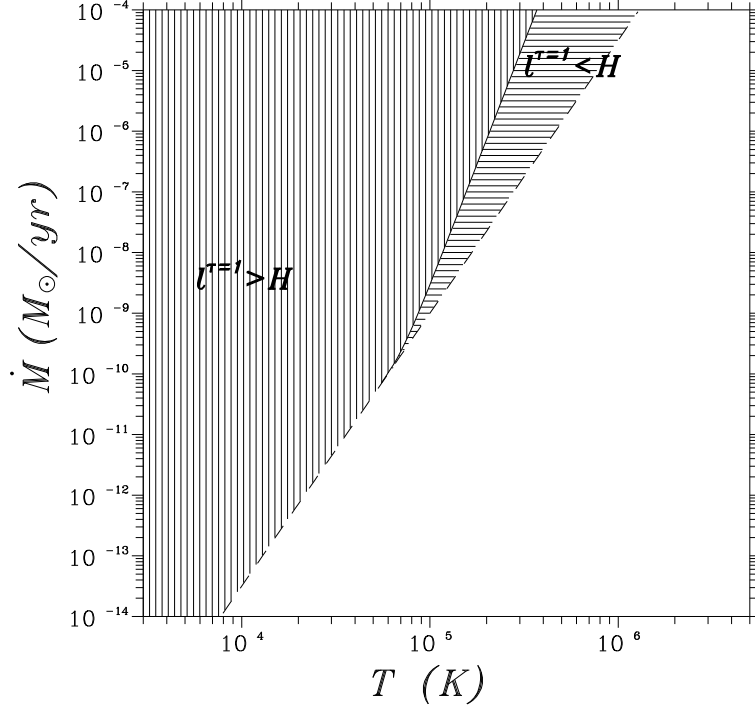


Figure 3: The same as Fig. 2 for disks with dominant radiation pressure.

responding to optically thin cool disks are possible for small  $\dot{M}$ . It follows from Fig. 3 that disks with dominant radiation pressure are mainly optically thin; optically thick hot disks can exist only for high  $\dot{M}$ .

## 2.4 Optically Thick Disks

In Section 2.2, we derived Eq. (7), which relates  $\dot{M}$ ,  $T$ , and  $\rho$  for given  $a$ ,  $r$  and  $\alpha$ . Using the supplementary heat-balance equations (1)–(2), we can reduce the number of unknowns and obtain the desired relation between  $\dot{M}$  and  $T$ .

The vertical temperature distributions in optically thick disks are described by the equation of radiative heat conduction with a source due to viscous heating (2), which can be written in the form

$$\frac{\partial e}{\partial t} = \frac{\partial}{\partial z} \left( \frac{1}{\kappa \rho} \frac{\partial}{\partial z} \left( \frac{1}{3} a c T^4 \right) \right) + \rho \alpha c_s^2 \Omega_K, \quad (11)$$

where  $e$  is the specific internal energy and  $c$  is the velocity of light. To solve (11), we must specify boundary conditions. Due to the symmetry of the problem, the temperature derivative in the equatorial plane must be zero; i.e.,  $T'|_{z=0} = 0$ .



The temperature at the upper boundary of the disk is specified by the condition  $\Gamma(T_*, T_{wd}) = \Lambda(T_*)$ . Though the functions  $\Gamma(T, T_{wd})$  and  $\Lambda(T)$  are complex, they are known and can be found in the literature (see, for example, [21–23]). The temperature derived by equating these functions (for a temperature of the central object (white dwarf) of  $T_{wd} = 70\,000$  K) is  $T(H) = T_* = 13\,600$  K.

The solution of (11) enters a stationary regime when the characteristic heat-conduction time

$$t_{diff} \simeq \frac{\mathcal{R}\kappa\rho^2 H^2}{acT^3}$$

is comparable to the time for viscous heating

$$t_{heat} \simeq \frac{\mathcal{R}T}{\alpha c_s^2 \Omega_K} \simeq \alpha^{-1} \Omega_K^{-1}.$$

Note that (11) can be integrated analytically in the steady-state case. Let us denote  $U = T^4$ ,  $U_* = T_*^4$ ,  $U_0 = U|_{z=0}$  and again assume that does not depend on  $z$ . Then,

$$\frac{d}{dz} \left( \frac{1}{\kappa\rho} \frac{d}{dz} \left( \frac{ac}{3} U \right) \right) = -\rho\alpha c_s^2 \Omega_K.$$

After integrating over  $z$ , we obtain

$$\frac{1}{\kappa\rho} \frac{d}{dz} \left( \frac{ac}{3} U \right) = -\rho\alpha c_s^2 \Omega_K z,$$

The integration constant is equal to zero, since  $U'|_{z=0} = 0$ . For convenience, we will transform this last equation to the form

$$\frac{1}{\kappa} \frac{dU}{dz} \equiv \frac{dB}{dz} = -\frac{3}{ac} \rho^2 \alpha c_s^2 \Omega_K z,$$

where the function  $B(U)$  is determined from the differential equation  $\frac{dB}{dU} = \frac{1}{\kappa(U, \rho)}$  and can be written in an analytical form if  $\rho$  is fixed. Integrating this last equation over  $z$ , we obtain

$$B(U) = B(U_*) + \frac{3}{2ac} \rho^2 \alpha c_s^2 \Omega_K (H^2 - z^2),$$

or, for  $z = 0$

$$B(U_0) = B(U_*) + \frac{3}{2ac} \rho^2 \alpha c_s^2 \Omega_K H^2.$$

Using the expressions

$$c_s^2 = \left( \mathcal{R}U_0^{1/4} + \frac{1}{3} \frac{aU_0}{\rho} \right),$$

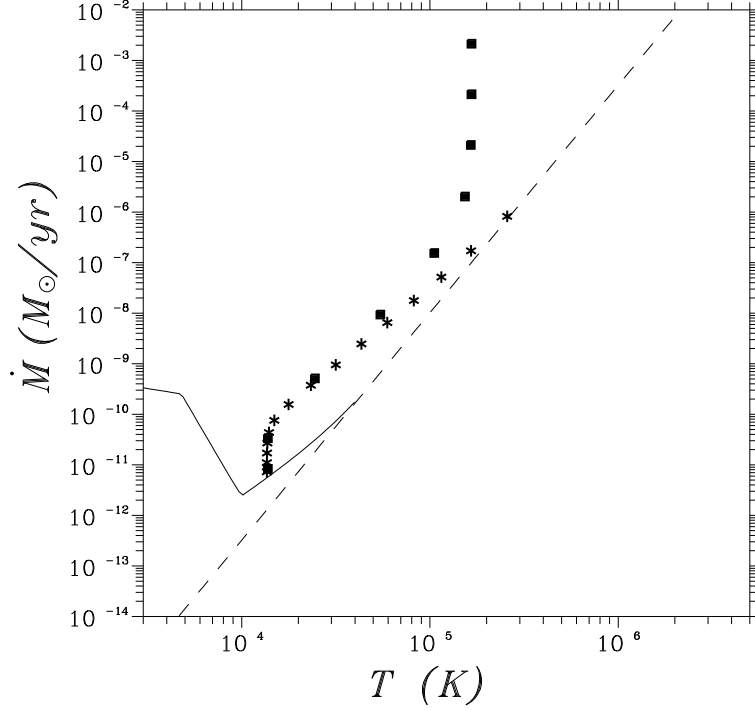


Figure 4: Solution of (11) for an optically thick disk for  $\alpha = 1$  and  $r = A/5$  (asterisks). Solutions of (12) taking into account convection are labeled by squares. The dashed line is a lower bound for the region in which there exist solutions of (7), and the solid line separates the regions of optically thin and optically thick disks.

$$H^2 = \left( \mathcal{R}U_0^{1/4} + \frac{1}{3}\frac{aU_0}{\rho} \right) \Omega_K^{-2}$$

we obtain the algebraic equation for  $U_0$

$$B(U_0) = B(U_*) + \frac{3}{2ac}\rho^2\alpha\Omega_K^{-1} \left( \mathcal{R}U_0^{1/4} + \frac{1}{3}\frac{aU_0}{\rho} \right)^2.$$

This equation implicitly specifies the dependence  $U_0(\rho)$ ; i.e.,  $T(\rho)$ . Expressing  $\dot{M}$  in terms of  $\rho$  and  $T$ , we can derive the dependence  $\dot{M}(\rho) = \dot{M}(T(\rho), \rho)$ , which yields the dependence  $T(\dot{M})$  in parametric form. Formally, the resulting solution can also exist in optically thin regions; however, given the adopted assumptions, these points can be rejected.

Let us consider a graphical representation of the solution derived. Figure 4 presents the dependence  $T(\dot{M})$  for  $\alpha = 1$  and  $r = A/5$ , marked by asterisks. As in Fig. 2–3, the dashed lines bound from below the domain in which there

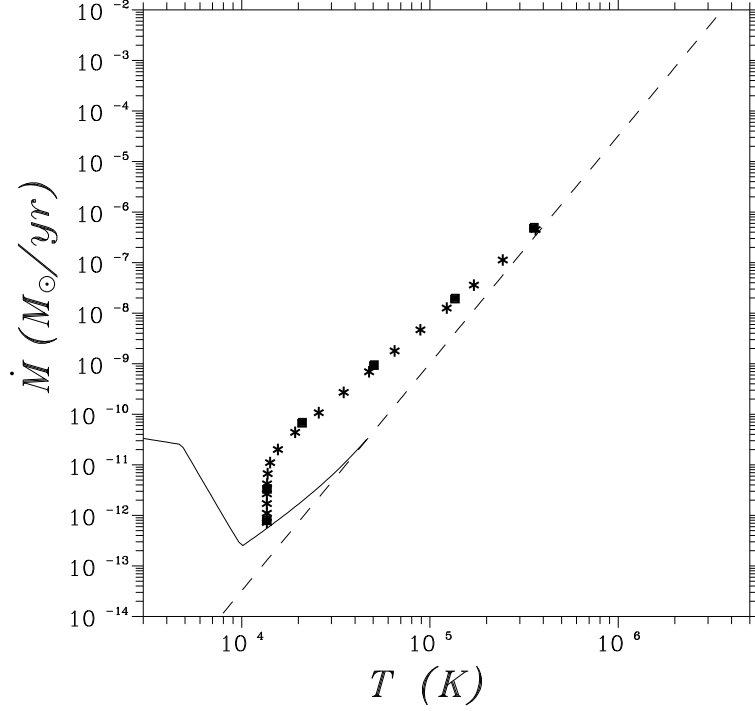


Figure 5: The same as Fig. 4 for  $\alpha = 0.1$ .

exist solutions of (7), while the solid line separates the domains of optically thin and optically thick disks. Figures 5–6 display the solutions for  $\alpha = 0.1$  and  $\alpha = 0.01$ , respectively. Figure 6 presents the accretion rate as a function of the disk thickness. We can see that all the obtained disks are geometrically thin; i.e.,  $H \ll r$ .

Radiative heat conduction is not the only mechanism for heat transfer into optically thin regions. Under certain conditions, convection can also play a substantial role. Neglecting the radiation pressure, the convective flux can be written in the form [24, 25]

$$F_{conv} = c_P \cdot \rho \cdot \left( \frac{|g|}{T} \right)^{1/2} \cdot \frac{l^2}{4} \cdot (\Delta \nabla T)^{3/2},$$

$$\Delta \nabla T = -\frac{T}{c_P} \cdot \frac{\partial S}{\partial z}.$$

Here,  $c_P$  is the heat capacity at constant pressure,  $S = \mathcal{R} \cdot \ln(T^{3/2}/\rho)$  the specific entropy,  $g = -\Omega_K^2 z$  the gravitational acceleration, and  $l$  the mixing length, taken to be  $l = \alpha H$ . To determine the vertical temperature distribution taking

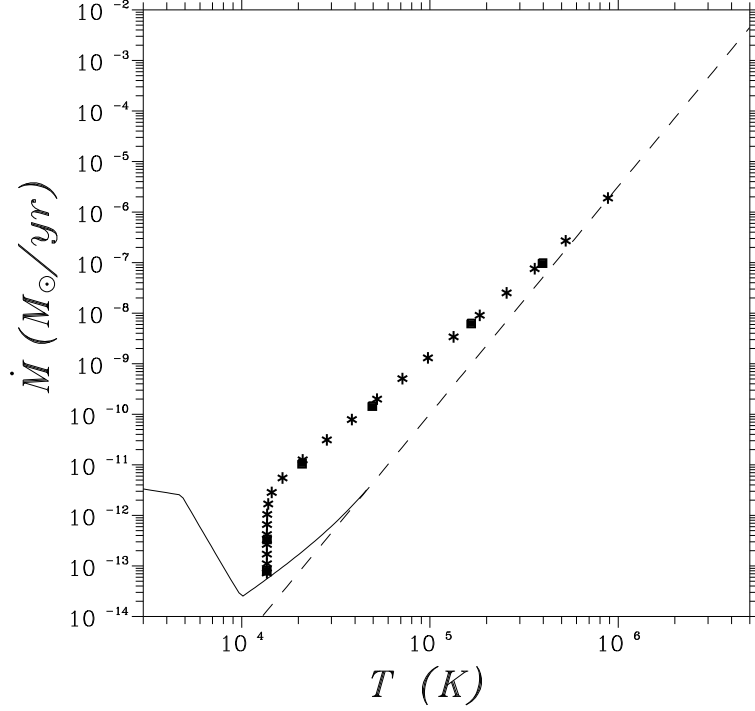


Figure 6: The same as Fig. 4 for  $\alpha = 0.01$ .

convection into account, we must solve the equation

$$\frac{\partial e}{\partial t} = \frac{\partial}{\partial z} \left( \frac{1}{\kappa \rho} \frac{\partial}{\partial z} \left( \frac{1}{3} a c T^4 \right) \right) - \frac{\partial F_{conv}}{\partial z} + \rho \alpha c_s^2 \Omega_K \quad (12)$$

with the same boundary conditions as for (11). Equation (12) does not admit a simple analytical solution, and we solved this equation numerically using the method of establishment. The solution is denoted by the squares in Figs.4–6. We can see that convection plays a significant role only when  $\alpha \simeq 1$ .

Summarizing, we can assert that, in the optically thick case with small  $\dot{M}$ , the disk displays the constant temperature  $T = T_* = 13600^\circ \text{ K}$ , while the temperature increases as  $T \propto \dot{M}^{1/3}$  at larger values of  $\dot{M}$ . Thus, for realistic parameters of the accretion disks in close binaries,  $\dot{M} \simeq 10^{-12} \div 10^{-7} M_\odot/\text{year}$  and  $\alpha \simeq 10^{-1} \div 10^{-2}$ , the gas temperature in the outer parts of the disk ( $r \simeq A/5 \div A/10$ ) is  $10^4 \text{ K}$  to  $\sim 10^6 \text{ K}$ .

Solving (11) for various  $r$ , we can also calculate the dependences  $T(r)$  and  $\rho(r)$ . The calculations indicate that  $T \propto r^{-0.8}$  and  $\rho \propto r^{-1.8}$ , which is consistent with the dependence  $T \propto r^{-3/4}$  obtained by Shakura and Sunyaev [26].

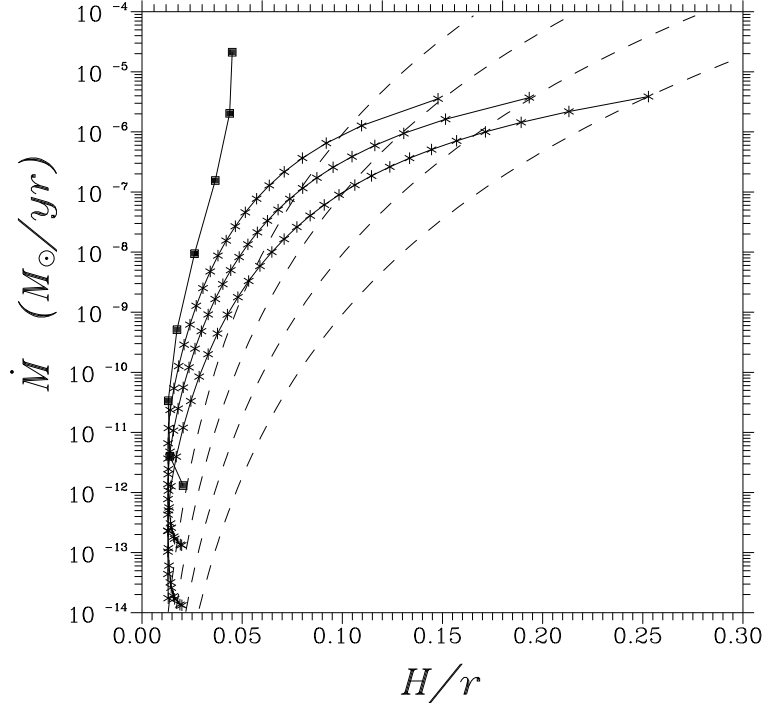


Figure 7: A disk with dominant gas pressure. The solid lines indicate possible states of the disk in the  $H/r - \dot{M}$  plane for  $r = A/5$ . Solutions of (11) taking into account radiative heat conduction and viscous heating are shown by the lines with asterisks for  $\alpha = 1$ ,  $\alpha = 0.1$ ,  $\alpha = 10^{-2}$ ,  $\alpha = 10^{-3}$  (top to the bottom). Solutions of (12) taking into account radiative heat conduction, convection, and viscous heating are shown by the lines with squares for  $\alpha = 1$ . The dashed lines bound from below regions in which the solution of (7) can exist for  $\alpha = 1$ ,  $\alpha = 0.1$ ,  $\alpha = 10^{-2}$ ,  $\alpha = 10^{-3}$  (top to bottom).

## 2.5 Optically Thin Disks

In this case, the temperature of the disk is specified by the balance between radiative heating  $\Gamma(T, T_{wd})$  and viscous heating (5), on the one hand, and radiative cooling  $\Lambda(T)$ , on the other. The heat-balance equation (1) can be written

$$\rho \alpha c_s^2 \Omega_K + \rho^2 \cdot m_p^2 \cdot (\Gamma(T, T_{wd}) - \Lambda(T)) = 0,$$

which can be reduced to the quadratic equations in  $\rho$

$$\alpha \cdot (\rho \mathcal{R}T + \frac{1}{3} a T^4) \cdot \Omega_K + \rho^2 \cdot m_p^{-2} \cdot (\Gamma(T, T_{wd}) - \Lambda(T)) = 0.$$

The solution of this equation for specified  $r$  and  $\alpha$  yields the dependence  $\rho(T)$ , and thus  $T(\dot{M})$ . Formally, this solution can also exist in optically thick regions, however these points were rejected by virtue of the adopted assumptions.

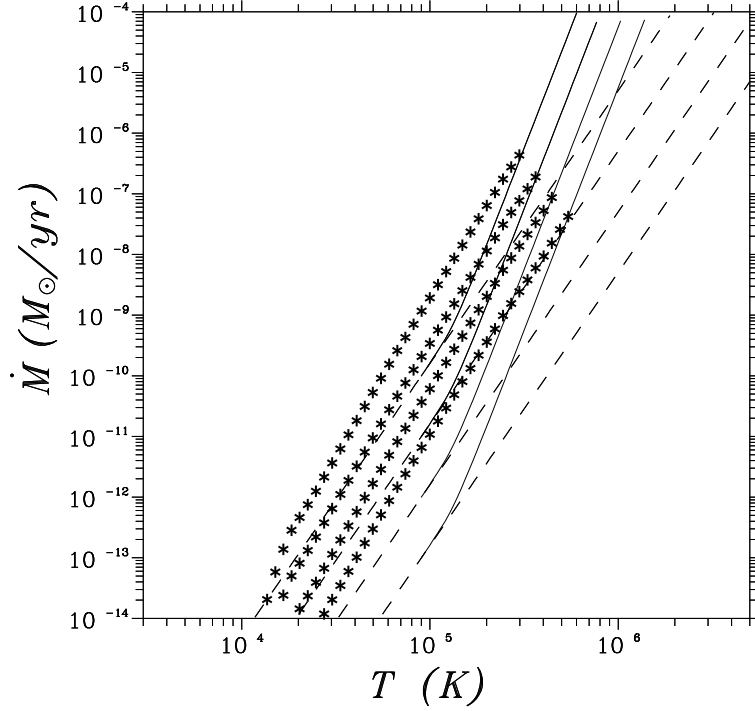


Figure 8: Solutions for an optically thin disk for  $\alpha = 1, \alpha = 0.1, \alpha = 10^{-2}, \alpha = 10^{-3}$  (top to bottom) and  $r = A/20$  (asterisks). The dashed lines bound from below the domain in which there exists a solution of (7); the solid lines separate the regions for optically thin and optically thick disks.

It is shown in Section 2.3 that disks in which gas pressure dominates are primarily optically thick, and solutions that correspond to optically thin disks are possible only for small  $\dot{M}$ . Disks in which radiation pressure dominates are primarily optically thin. The domination of radiation pressure is possible only in the inner parts of the disk; therefore, we will adopt  $r = A/20$  for the further analysis. For the typical dwarf nova IP Peg, this corresponds to five radii of the accretor (white dwarf).

Figure 8 presents the results of our calculations; the asterisks denote the  $T(\dot{M})$  dependences for  $\alpha = 1, \alpha = 0.1, \alpha = 10^{-2}, \alpha = 10^{-3}$  (top to bottom), and  $r = A/20$ . The disks obtained in these solutions are geometrically thick,  $H \simeq r$ . Note that the initial assumptions of the model restrict its applicability: it is suitable only for geometrically thin disks, and the solutions for geometrically thick disks are purely formal.

### 3 The Model

We described the flow structure in a binary system using a system of gravitational gas-dynamical equations taking into account radiative heating and cooling of the gas for the optically thin case:

$$\left\{ \begin{array}{l} \frac{\partial \rho}{\partial t} + \operatorname{div} \rho \mathbf{v} = 0, \\ \frac{\partial \rho \mathbf{v}}{\partial t} + \operatorname{div}(\rho \mathbf{v} \otimes \mathbf{v}) + \operatorname{grad} P = -\rho \operatorname{grad} \Phi, \\ \frac{\partial \rho(\varepsilon + |\mathbf{v}|^2/2)}{\partial t} + \operatorname{div} \rho \mathbf{v}(\varepsilon + P/\rho + |\mathbf{v}|^2/2) = \\ \quad = -\rho \mathbf{v} \operatorname{grad} \Phi + \rho^2 m_p^{-2} (\Gamma(T, T_{wd}) - \Lambda(T)). \end{array} \right. \quad (13)$$

Here, as usual,  $\rho$  is the density,  $\mathbf{v} = (u, v, w)$  the velocity vector,  $P$  the pressure,  $\varepsilon$  the internal energy,  $\Phi$  the Roche gravitational potential,  $m_p$  the proton mass, and  $\Gamma(T, T_{wd})$  and  $\Lambda(T)$  the radiative heating and cooling functions, respectively. The system of gas-dynamical equations was closed with the Clapeyron equation  $P = (\gamma - 1)\rho\varepsilon$ , where  $\gamma$  is the adiabatic index. We took the parameter  $\gamma$  to be 5/3.

Our main goal here is to study the morphology of the interaction between the stream and the cool accretion disk. It follows from Section 2 that the outer parts of the accretion disk can be cool for small  $\dot{M}$  and, in particular, in the case of an optically thin disk. The system of equations (13) enables us to carry out three-dimensional modeling of the flow structure in a binary within our formulation of the problem. In the model, the temperature of the disk is 13 600 K.

We solved this system of equations using the Roe-Osher method [14, 27, 28], adapted for multiprocessing computations via spatial decomposition the computation grid (i.e., partitioning into subregions, with synchronization of the boundary conditions) [29]. We considered a semi-detached binary system containing a donor with mass  $M_2$  filling Roche lobe and an accretor with mass  $M_1$ . The system parameters were specified to be those of the dwarf nova IP Peg:  $M_1 = 1.02M_\odot$ ,  $M_2 = 0.5M_\odot$ ,  $A = 1.42R_\odot$ .

The modeling was carried out in a non-inertial reference frame rotating with the binary, in Cartesian coordinates in a rectangular three-dimensional grid. Since the problem is symmetrical about the equatorial plane, only half the space occupied by the disk was modeled. To join the solutions, we specified a corresponding boundary condition at the lower boundary of the computation domain. The accretor had the form of a sphere with radius  $10^{-2}A$ . All matter that ended up within any of the cells forming the accretor was taken to fall onto the star. A free boundary condition was specified at the outer boundaries of the disk – the density was

constant ( $\rho_b = 10^{-8}\rho_{L_1}$ ), where  $\rho_{L_1}$  is the density at the point  $L_1$ , the temperature was 13 600 K, and the velocity was equal to zero. The stream was specified in the form of a boundary condition: matter with temperature 5800 K, density  $\rho_{L_1} = 1.6 \times 10^{-8} g/cm^3$  and velocity along the  $x$  axis  $v_x = 6.3 km/s$  was injected into a zone around  $L_1$  with radius  $0.014A$ . For this rate of matter input into the system, the model accretion rate was  $\sim 10^{-12} M_\odot/year$ .

The size of the computation domain,  $1.12A \times 1.14A \times 0.17A$ , was selected so that it entirely contains both the disk and stream, including the point  $L_1$ . The computation grid with  $121 \times 121 \times 62$  cells was distributed between 81 processors, which constituted a two-dimensional  $9 \times 9$  matrix.

To increase the accuracy of the solution, the grid was made denser in the zone of interaction between the stream and disk, making it possible to resolve well the formed shock wave. The grid was also denser towards the equatorial plane, so that the vertical structure was resolved, even for such a cool disk.

We used the solution obtained for a model without cooling as the initial conditions [12]. The model with cooling was computed during approximately five revolutions of the system, until the solution became established. The total time of the computations was  $\approx 1000$  h on the MBC1000A computer of the Joint Supercomputer Center (JSC).

## 4 Computation Results

Figures 9 to 13 present the morphology of gas flows in the binary. Figure 9 shows the density and velocity vector distributions in the equatorial plane of the system (the  $XY$  plane), while Figs. 10 and 11 present density contours in the frontal ( $XZ$ ) plane and in the  $YZ$  plane containing the accretor and perpendicular to the line connecting the binary components. In spite of the small height of the forming accretion disk, use of the JSC parallel-processing computers made it possible to resolve its vertical structure (the outer parts of the disk were covered by 15 grid cells, and the inner parts by no fewer than 3 cells). Figure 12 gives an enlarged view of the density and velocity vector distributions in the zone of interaction between the stream and the outer edge of the disk (the area in the shaded rectangle in Fig. 9). Figure 13 presents the so-called texture a visualization of the velocity field in the zone of interaction between the stream and disk, constructed using the Line Integral Convolution procedure (LIC) [30].

According to our considerations in [8, 14], the gasdynamical flow pattern in a semi-detached binary is formed by the stream from  $L_1$ , the disk, a circumdisk halo, and the intercomponent envelope. This subdivision is based on physical differences between these elements of the flow structure: (1) if the motion of the gas is not determined by the gravitational field of the accretor, it forms the intercom-



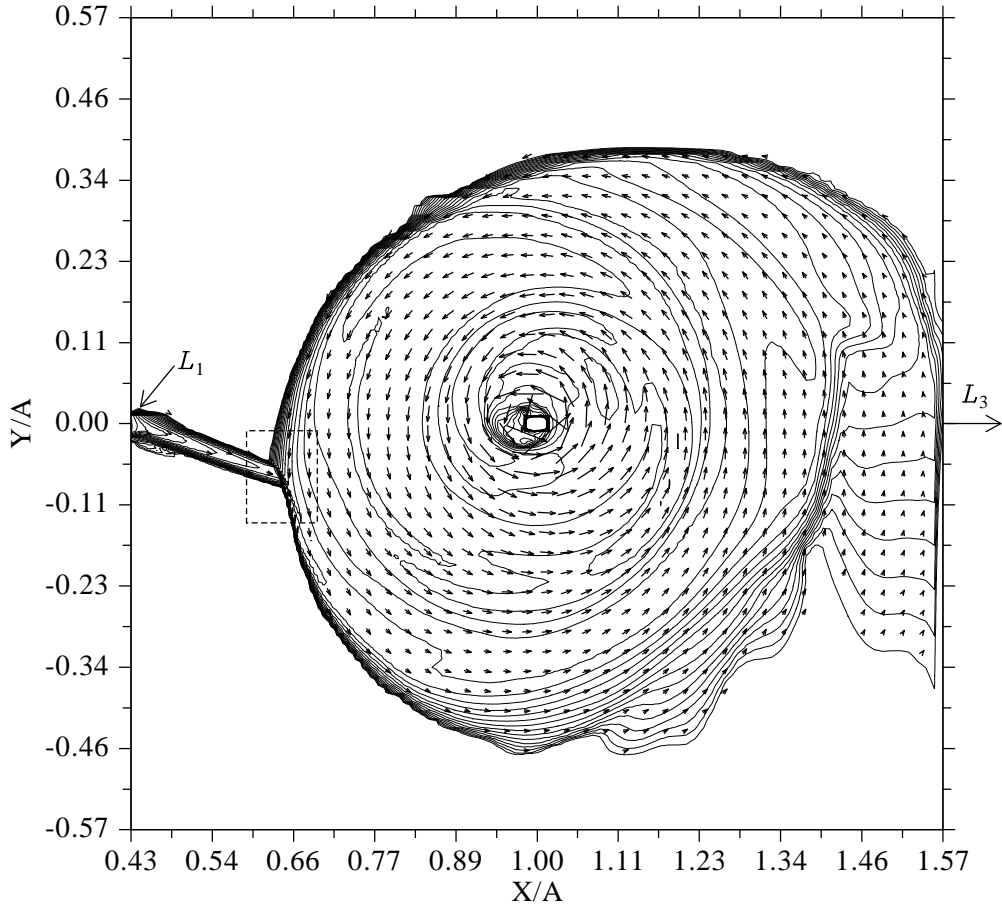


Figure 9: Contours of constant density and velocity vectors in the equatorial plane  $XY$  of the system. The shaded rectangle indicates the zone of interaction between the stream and disk, shown in Figs 12 and 13. The point  $L_1$  and the direction towards  $L_3$  are marked.

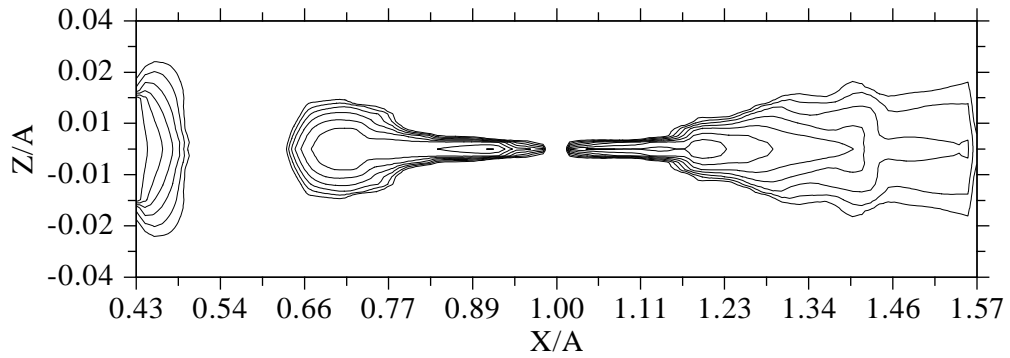


Figure 10: Density contours in the frontal plane  $XZ$  of the system.

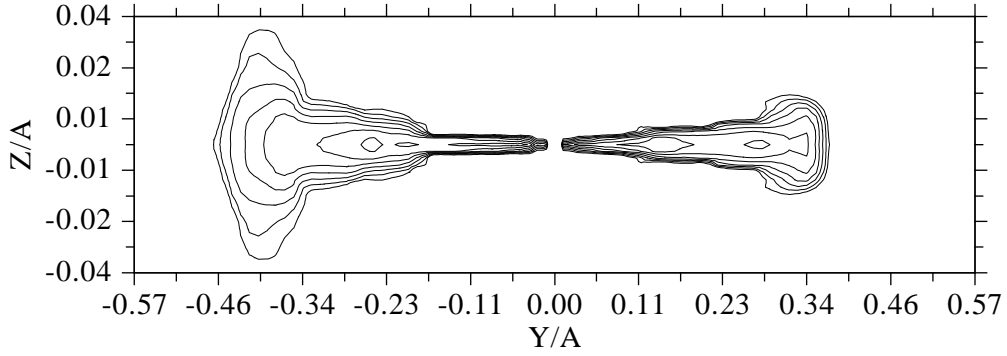


Figure 11: Density contours in the plane  $YZ$  containing the accretor and perpendicular to the line connecting the binary components.

ponent envelope; (2) if the gas makes one revolution around the accretor, but later mixes with the initial stream, this gas does not become part of the disk, instead forming the circum-disk halo; (3) the disk is formed by that part of the stream that loses its momentum and moves towards the center of gravity after entering the gravitation field of the accretor, rather than interacting with the stream.

In this framework, let us consider the morphology of the flow when the temperature decreases to 13 600 K over the entire computation domain due to cooling. Figure 9 indicates that, in this case, the intercomponent envelope is formed primarily in the vicinity of  $L_3$ , and does not affect the solution substantially. We can see from Figs. 9 and 10–11 that the circum-disk halo is pressed against the disk, and its density increases sharply towards the disk edge.

Figures 12 and 13 show that, in the cool-disk case, the interaction between the circum-disk halo and the stream displays all features typical of an oblique collision of two streams. We can clearly see two shock waves and a tangential discontinuity between them. The gases forming the halo and stream pass through the shocks corresponding to their flows, mix, and move along the tangential discontinuity between the two shocks. Further, this material forms the disk itself, the halo, and the envelope.

The solution for the cool case displays the same qualitative characteristics as the solution for the case when the outer parts of the disk are hot: the interaction between the stream and disk is shockless, a region of enhanced energy release is formed due to the interaction between the circum-disk halo and the stream and is located beyond the disk, and the resulting shock is fairly extended, which is particularly important for explaining the observations. However, unlike the solution with a high temperature in the outer regions of the disk [1, 12, 14], in the cool case, the shape of the zone of shock interaction between the stream and halo is more complex than a simple “hot line”. This is due to the sharp increase of the

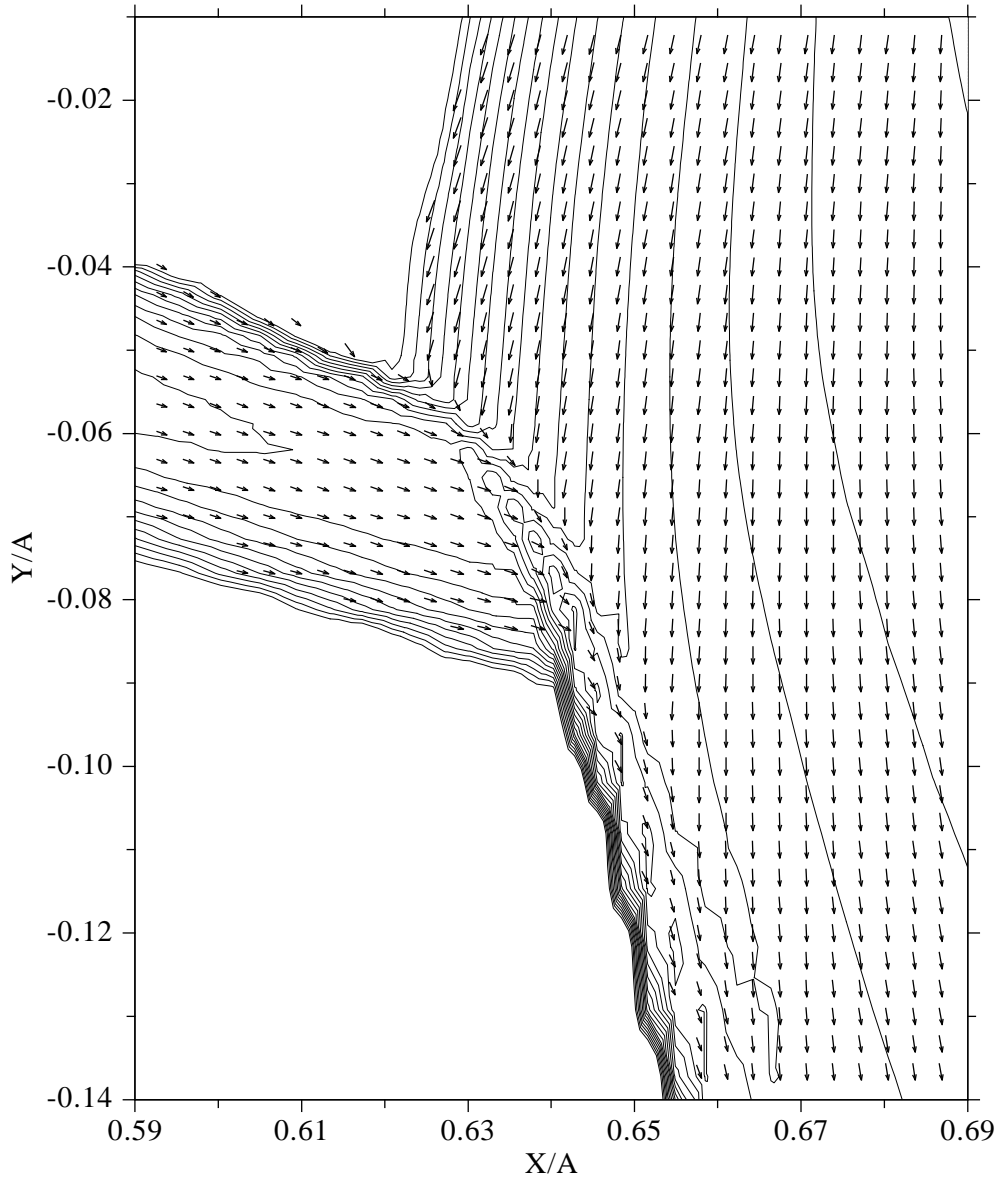


Figure 12: Contours of constant density and velocity vectors in the zone of interaction between the stream and disk (the shaded rectangle in Fig. 9).

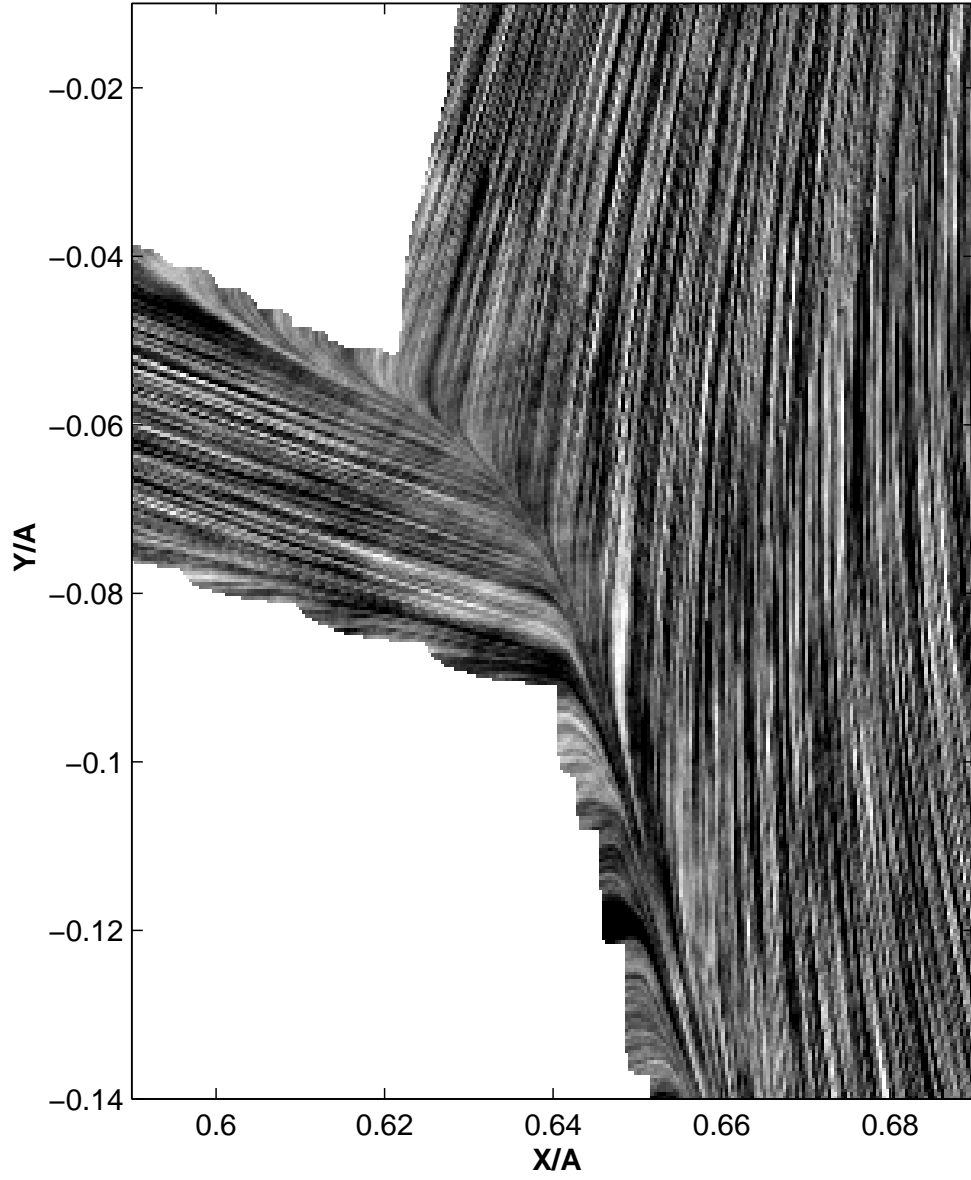


Figure 13: Visualization of the velocity field in the zone of interaction between the stream and disk (the shaded rectangle in Fig. 9).

halo density as the disk is approached. Those parts of the halo that are far from the disk have low density, and the shock due to their interaction with the stream is situated along the edge of the stream. As the halo density increases, the shock bends, and eventually stretches along the edge of the disk.

## 5 Conclusions

Our analysis of the basic processes of heating and cooling in accretion disks in binaries has shown that, for realistic parameters of the accretion disks in close binary systems ( $\dot{M} \simeq 10^{-12} \div 10^{-7} M_{\odot}/year$  and  $\alpha \simeq 10^{-1} \div 10^{-2}$ ), the gas temperature in the outer parts of the disk is  $10^4$  K to  $\sim 10^6$  K.

Previously, we carried out three-dimensional simulations of the flow structure in close binaries for the case when the temperature of the outer parts of the accretion disk was 200–500 thousand K. Those solutions showed that the interaction between the stream from the inner Lagrange point and the disk was shockless. To determine the generality of the solution, the morphology of the flow for different disk temperatures must be considered. We have presented here the results of simulations for the case when cooling decreases the temperature to 13 600 K over the entire computation domain.

Our analysis of the flow pattern for the cool outer parts of the disk confirms that the interaction between the stream and disk is again shockless. The computations indicate that the solution for the cool disk case displays the same qualitative features as in the case when the outer parts of the disk are hot: the interaction between the stream and disk is shockless, a region of enhanced energy release formed by the interaction between the circum-disk halo and the stream is located beyond the disk, and the shock wave that is formed is fairly extended, and can be considered a “hot line”. The cool solution demonstrates the universal character of our previous conclusions that the interaction between the stream and disk in semidetached binaries is shockless.

## 6 Acknowledgments

This work was supported by the Russian Foundation for Basic Research (project codes 02-02-16088, 02-02-17642), the State Science and Technology Program in Astronomy, a Presidential Grant of the Russian Federation (00-15-96722), the Programs of the Presidium of the Russian Academy of Sciences “Mathematical Modeling” and “Non-steady State Processes in Astronomy”, and the INTAS Foundation (grant 01-491).

## References

- [1] D. V. Bisikalo, A. A. Boyarchuk, O. A. Kuznetsov, and V. M. Chechetkin, *Astron. Zh.* **74**, 880 (1997) [*Astron. Rep.* **41**, 786 (1997)].
- [2] D. V. Bisikalo, A. A. Boyarchuk, O. A. Kuznetsov, and V. M. Chechetkin, *Astron. Zh.* **74**, 889 (1997) [*Astron. Rep.* **41**, 794 (1997)].
- [3] D. V. Bisikalo, A. A. Boyarchuk, O. A. Kuznetsov, and V. M. Chechetkin, *Astron. Zh.* **75**, 706 (1998) [*Astron. Rep.* **42**, 621 (1998)].
- [4] D. V. Bisikalo, A. A. Boyarchuk, V. M. Chechetkin, et al., *Mon. Not. R. Astron. Soc.* **300**, 39 (1998).
- [5] D. V. Bisikalo, A. A. Boyarchuk, O. A. Kuznetsov, and V. M. Chechetkin, *Astron. Zh.* **76**, 270 (1999) [*Astron. Rep.* **43**, 229 (1999)].
- [6] D. V. Bisikalo, A. A. Boyarchuk, O. A. Kuznetsov, and V. M. Chechetkin, *Astron. Zh.* **76**, 672 (1999) [*Astron. Rep.* **43**, 587 (1999)].
- [7] D. V. Bisikalo, A. A. Boyarchuk, O. A. Kuznetsov, and V. M. Chechetkin, *Astron. Zh.* **76**, 905 (1999) [*Astron. Rep.* **43**, 797 (1999)].
- [8] D.V.Bisikalo, A.A.Boyarchuk,O.A.Kuznetsov, and V. M. Chechetkin, *Astron. Zh.* **77**, 31 (2000) [*Astron. Rep.* **44**, 26 (2000)].
- [9] D. Bisikalo, P. Harmanec, A. Boyarchuk, et al., *Astron. Astrophys.* **353**, 1009 (2000).
- [10] D. V. Bisikalo, A. A. Boyarchuk, A. A. Kilpio, et al., *Astron. Zh.* **78**, 707 (2001) [*Astron. Rep.* **45**, 611 (2001)].
- [11] D. V. Bisikalo, A. A. Boyarchuk, A. A. Kilpio, and O. A. Kuznetsov, *Astron. Zh.* **78**, 780 (2001) [*Astron. Rep.* **45**, 647 (2001)].
- [12] O. A. Kuznetsov, D. V. Bisikalo, A. A. Boyarchuk, et al., *Astron. Zh.* **78**, 997 (2001) [*Astron. Rep.* **45**, 872 (2001)].
- [13] D. Molteni, D. V. Bisikalo, O. A. Kuznetsov, and A. A. Boyarchuk, *Mon. Not. R. Astron. Soc.* **327**, 1103 (2001).
- [14] A. A. Boyarchuk, D. V. Bisikalo, O. A. Kuznetsov, and V. M. Chechetkin, *Mass Transfer in Close Binary Stars* (Taylor and Francis, London, 2002).
- [15] N. I. Shakura, *Astron. Zh.* **49**, 921 (1972) [*Sov. Astron. Rep.* **6**, 756 (1972)].

- [16] D. N. Lin and J. Papaloizou, *Mon. Not. R. Astron. Soc.* **91**, 37 (1980).
- [17] D. R. Alexander, G. C. Augason, and H. R. Johnson, *Astrophys. J.* **45**, 1014 (1989).
- [18] K. R. Bell and D. N. C. Lin, *Astrophys. J.* **27**, 987 (1994).
- [19] J. K. Cannizzo and S. J. Kenyon, *Astrophys. J. Lett.* 309, L43 (1986).
- [20] E. Meyer-Hoffmeister and H. Ritter, in *The Realm of Interacting Binary Stars*, Ed. by J. Sahade, G. E. McCluskey, Jr., and Y. Condo (Kluwer Acad., Dordrecht, 1993), p. 143.
- [21] D. P. Cox and E. Daltabuit, *Astrophys. J.* **67**, 113 (1971).
- [22] J. C. Raymond, D. P. Cox, and B. W. Smith, *Astrophys. J.* **04**, 290 (1976).
- [23] L. Spitzer, Jr., *Physical Processes in the Interstellar Medium* (Wiley, New York, 1978; Mir, Moscow, 1981).
- [24] M. Schwarzschild, *Structure and Evolution of the Stars* (Princeton Univ. Press, Princeton, 1958; Inostr. Lit., Moscow, 1961).
- [25] G. S. Bisnovaty-Kogan, *Physical Processes in the Theory of Stellar Evolution* (Nauka, Moscow, 1989; Springer, Berlin, 2001) [in Russian].
- [26] N. I. Shakura and R. A. Sunyaev, *Astron. Astrophys.* **4**, 337 (1973).
- [27] P. L. Roe, *Ann. Rev. FluidMech.* **8**, 337 (1986).
- [28] S. R. Chakravarthy and S. Osher, *AIAA Pap.* No. **85**- 0363 (1985).
- [29] P. V. Kaigorodov and O. A. Kuznetsov, Preprint 59, Keldysh Inst. App. Math., Rus. Acad. Sci. (Moscow, 2002).
- [30] B. Cabral and C. Leedom, in *ACM SIGGRAPH, Computer Graphics Proceedings 93*, (1993), p. 263.